Structures 56 (2023) 104875

Contents lists available at ScienceDirect

Structures

journal homepage: www.elsevier.com/locate/structures

Influences of random imperfection distribution on the compressive properties of interlocking block wall

Tingwei Shi [a], Xihong Zhang [a,*], Hong Hao [a,b], Guanyu Xie [a]

[a] Centre for Infrastructural Monitoring and Protection, School of Civil and Mechanical Engineering, Curtin University, Bentley, WA 6102, Australia
[b] Earthquake Engineering Research and Test Centre, Guangzhou University, Guangzhou, China

ARTICLE INFO

Keywords:
Interlocking blocks
Imperfection
Monte-Carlo simulations
Spatial variability
Seating effect

ABSTRACT

Block imperfections exist inevitably owing to manufacturing and construction quality control. For dry-stacked interlocking block structures, imperfections result in small gaps randomly distributed between blocks, which affect the compressive strength of the wall. In this study, stochastic analysis is conducted to predict the compressive properties of interlocking block walls with spatially varying randomly distributed block imperfections. Monte-Carlo simulation is conducted in the analysis. The number of block imperfections is assumed to follow the Binominal distribution in massive block production process; the imperfection sizes are assumed to follow the truncated normal distribution. Based on these hypotheses, the damage development mechanism and load-path of interlocking block walls with different imperfection distributions are investigated. It is found that the compressive strength of walls containing blocks with mixed imperfection levels is lower; for walls with a higher number of imperfections, a larger coefficient of variation of imperfections leads to a significant decrease in compressive strength, while the seating effect at the initial stage of compression is reduced. The results provide a guidance to the quality control of mortar-less interlocking block structures.

1. Introduction

Masonry structures are popularly constructed because of their relatively low cost and good thermal performance. To improve the structural performance, construction efficiency and quality, interlocking blocks, which have interlocking keys resembling the shear keys in prefabricated concrete structures and share similar advantages [1], have been introduced over the past decades and demonstrated outstanding structural performance [2–4]. Mortar-less (dry-stacking) and/or thin-bed mortar joining methods have also been developed for fast-laying block products. Combining interlocking block with mortar-less construction method is very attractive for masonry structures. Nevertheless, unlike prefabricated concrete structures, which have been used for a long time and whose mechanical performance has been studied under varying circumstances [5,6], the influence of surface roughness or imperfection of interlocking blocks on the structural performance of mortarless interlocking block walls has not been properly studied and explicitly understood yet. Unlike the traditional masonry constructions where the imperfections on block surfaces are remedied by mortar that joins the adjacent blocks, the imperfections of blocks in mortar-less masonry structure result in gaps between interlocking blocks, which affect the structural strength, stiffness, and deformation capacities. Therefore, the influences of imperfections on the performances of interlocking block structures should be investigated. Moreover, as the mechanical properties depend on the design of interlocking keys, which varies from one design to another. There is no design standard or recommended practice for the design of mortar-less interlocking block wall in engineering applications yet.

In practical applications, masonry structures are mainly subjected to vertical compressive loading from dead load and live load [7]. Therefore, it is most important to properly and accurately predict the compressive capacity of masonry walls constructed with interlocking blocks using mortar-less method. Some laboratory tests have been carried out to examine the compressive behaviour of interlocking block prisms and wallets with different designs of interlocking blocks. For instance, Sturm et al. [8] experimentally investigated the behaviour of prisms and wallets made of stabilized interlocking compressed earth blocks. Ngapeya et al. [9] carried out both experimental tests and numerical modelling to investigate the influence of geometrical imperfections on the compressive strength of one type of dry-stacked masonry walls. Jaafar et al. [10] found that contacting behaviour between the dry joints of interlocking blocks presented nonlinear progressive closure

* Corresponding author.
E-mail address: xihong.zhang@curtin.edu.au (X. Zhang).

https://doi.org/10.1016/j.istruc.2023.104875
Received 21 February 2023; Received in revised form 6 June 2023; Accepted 10 July 2023
Available online 25 July 2023

when the wall was subjected to gradually increased compressive load. Al-Fakih et al. [11] conducted compressive tests on dry-stacked interlocking masonry prisms, wallets and panels. It was found that the imperfections on the contacting interfaces considerably reduced the contact stiffness of the bed joints. Dorji et al. [12] found that compressive cracks in ungrouted dry-stacked masonry would not be transmitted to the bottom masonry units due to the mortarless feature and the lower overall stiffness of the dry-stacked masonry comparing to mortar-bonded masonries. Zahra et al. [13] carried out compressive tests on dry-stacked interlocking masonry panels and found that grouting could significantly enhance the compressive strength of mortarless masonry and reduce the seating effect. Many numerical studies have also been carried out based on both the simplified linear analysis and detailed nonlinear finite-element modellings to analyse the compressive capacity and failure mechanisms of interlocking prisms, wallets and walls [14–21]. The influences of some design parameters, such as the block material strength, prism/wallet height and block geometry on the compressive capacity and deformation capacity of dry-stacked interlocking prisms and wallets have also been studied.

Imperfection unavoidably exists in dry-stacked interlocking blocks resulted from block manufacturing error/tolerance and the quality of workmanship. For conventional clay blocks or concrete masonry units bonded with mortar, these imperfections could be mitigated by the mortar layer, which nevertheless does not exist in mortar-less/dry-stacking construction of interlocking blocks. It has been found that imperfections will not only affect the local strength and stiffness of interlocking blocks [19] but also influence the overall behaviour of structures made of interlocking blocks [22,23]. Therefore, it is necessary to properly evaluate the influence of imperfection on interlocking block structures constructed with the mortar-less method.

Previous laboratory tests found that imperfections of block units could result in seating effect when masonry piers/walls are subjected to compressive load [24–27]. Some researchers took block imperfection into considerations when numerically modelling the compressive behaviour of masonry structures. For instance, Shi et al. [19] employed different modelling strategies to consider the gaps at block joints associated with the block imperfections for interlocking block prism. It was found that such imperfections would strongly influence the compressive behavior of interlocking block prisms. Nevertheless, previous studies only considered non-spatial variability of imperfections in which the same imperfection was assumed throughout the block pier/wall. This simplification apparently would not properly represent the real condition of block structures, where the size of imperfection of each block unit varies; the locations of these imperfections also vary across the structure [28]. Therefore, a proper study that considers the random spatial variations of imperfection of each block and location within a structure should be performed.

Stochastic analysis has been commonly used to investigate the influences of random variables on structural performance of masonry structures [29–31]. For example, the influence of material uncertainties on the axial compressive strength of masonry wallets was investigated through probability analysis based on Monte-Carlo simulations [32]. Stewart and Lawrence [33] generated a probabilistic model to assess the structural reliability of masonry walls subjected to concentrically compressive loading considering variations in mortar type, live-to-dead load ratio, block material compressive strength and tributary area. The accuracy of design code, i.e., the Australian masonry design code AS3700-2001 [34], was examined based on the reliability analysis. Existence of spatial variability of block joint flexural bond-wrench strengths was also studied using stochastic analysis. For example, the influence of spatial correlation among unit block joint flexural bond-wrench strengths was experimentally studied by Heffler et al. [35]. It was found that the flexural bond-wrench strength of each block unit is statistically independent of its neighbouring unit. Li et al. [36] found that there are obvious differences between spatial and non-spatial analysis of the flexural bond-wrench strength of block wall in terms of wall performance and failure mode. Non-spatial simulation was found to overestimate the mean of wall compressive strength compared with spatial simulation. Some previous studies also investigated the influence of workmanship quality on the strength of masonry structures [37,38]. For instance, Stewart and Lawrence [38] studied the effect of workmanship quality, discretising of masonry unit thickness and wall width on the reliability index. It was concluded that the structural reliabilities are very susceptible to the workmanship quality, discretising of masonry unit thickness and wall width. Martínez et al. [16] discussed the impacts of random variation in the rough surfaces of block. Shi et al. [19] investigated that the compressive behavior of interlocking prisms comprised of interlocking block with non-spatially varied imperfections. No seating effect was observed in the numerical simulation. Ngapeya et al. [9] estimated the load bearing capacity considering the height imperfection of each block. It was found that the height imperfection of individual block plays a critical role in the failure mechanism and load bearing performance of a dry-stacked block wall subjected to compressive load. This is because the height imperfection controls the actual contacting area between the neighbouring masonry courses, and thus it dominates the load percolation system in the wall. Gooch et al. [39] established finite-element models of masonry structures, and found the numerical modellings tend to overestimate the elastic stiffness of laboratory structures. Therefore, it is necessary to properly understand and interpret the numerical modelling results. Till now, only very few studies investigated the structural performance of dry-stacked interlocking structures with consideration of the spatial variation of imperfections. Critical structure performance factors such as the stiffness and compressive strength of dry-stacked interlocking block wall are not understood well yet.

This study presents numerical investigations on the compressive behaviour of dry-stacked interlocking block wallets using stochastic analysis considering spatial variability of block imperfection. Monte-Carlo simulations are carried out to examine the influence of different number of block imperfections, imperfection locations in a wallet and varying imperfection sizes. The quality of interlocking block walls is categorized according to the number of imperfect blocks, while the coefficient of variation (COV) of the block imperfection is employed to represent dispersion of imperfections. Stress–strain curves and failure progression are examined. The variability of load carrying capacity, stiffness and damage mode are studied for interlocking block walls with different qualities. It should be noted that this study does not intend to research on stochastic methods, but uses existing method to investigate the influences of random interlocking block imperfections on masonry wall load carrying capacities. The novelty and significance of this study reside in its pioneering stochastic analysis of the compressive properties of dry-stacked interlocking block walls considering spatially varying block imperfections. This research innovatively models these imperfections using Binominal and truncated normal distributions for the number and sizes of imperfections, respectively. The examination of the influence of imperfection distributions on the damage development mechanism and load-path of interlocking block walls fills a gap in the existing literature. This approach not only enhances the accuracy of compressive strength prediction but also furnishes critical insights for improving quality control in mortar-less interlocking block structures. By bolstering the understanding of the impacts of block imperfections on structural performance, this study contributes significantly to the scientific robustness of construction methods involving dry-stacked interlocking blocks.

2. Numerical model

2.1. Block configuration

Fig. 1 illustrates the interlocking blocks considered in this study. Inspired by the osteomorphic block [40], the studied block achieves topological interlocking through concavoconvex surfaces (i.e., the

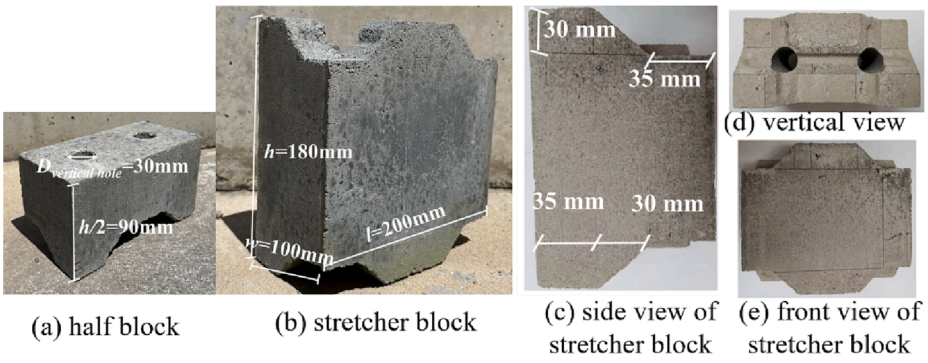

Fig. 1. Configuration of interlocking blocks.

tenons and mortises on the blocks). Thus, compared with other common interlocking masonry units that achieve interlocking through special connectors, this type of block can be assembled into complex structures with single or multiple layers [41]. Previous study [41] showed that when structures made of this type of block are damaged, the damage tends to be confined to individual blocks, rather than leading to global failure as in solid structures. Also, because the interlocking mechanism between these blocks is achieved through tenons and mortises distributed in various positions on the blocks, stress concentration at joints can be largely avoided [40,41].

As shown in Fig. 1, the block has a width of 200 mm, a height of 180 mm and a thickness of 100 mm. Asymmetric interlocking shear keys are designed for the block, where on the frontal side there is a wide shear key with a dimension of 70 mm width × 30 mm height × 35 mm, and on the rear side there are two smaller keys with geometric dimensions of 35 mm width × 30 mm height × 35 mm. The configuration of interlocking blocks is designed to provide improved shear resistance which differs from other existing interlocking blocks whose interlocking keys are usually only for self-alignment. The shear keys have inclined surfaces, which make the block assembly easier and allows the blocks to slide on each other under high lateral force. The material of blocks is a mixture composed of sand, cement, gravel, and fly ash, therefore it has properties similar to those of concrete.

2.2. Finite element model

2.2.1. Model detail

A detailed three dimensional finite element model of interlocking wall with dimension 1200 mm × 800 mm × 100 mm (height × width × thickness) is constructed using the commercial software Abaqus [42]. As mentioned above, interlocking blocks are modelled using solid element C3D8R with the Concrete Damage Plasticity (CDP) material model, in which both block crushing in compression and cracking in tension can be considered. The material properties of the interlocking block are shown in Table 1, where E_0 and ν denote the Young's modulus and the Poisson's ratio. More detailed modelling of the interlocking block properties and the corresponding verification can be referred to [43]. The compressive strength of block material is 17.46 MPa [43]. The tensile strength is assumed as $f_t = 0.1\ f_c$, which is a relationship commonly employed for concrete material [16,44].

2.2.2. Boundary condition and contact properties

For the interlocking block wall, the bottom surface of the wall is fully fixed, and the lateral and rotational movements (out-of-plane) at the top of the wall are restrained while its vertical degree of freedom is enabled for the application of the vertical loading. Displacement-controlled method is used to load the interlocking block wall till failure.

A hard contact is employed to model the contact behavior between adjacent blocks in the normal direction that the normal stress is transferred through the two surfaces. The contact surfaces will separate from each other when subjected to a normal tensile force; hence no tensile stress will be transferred across the contact surfaces. The contact behavior in the tangential direction of the interface is simulated using a finite sliding model following the Coulomb friction law. The tangential movement initiates when the surface traction stress at the connecting interface reaches the threshold shear strength τ, which is governed by the normal contact pressure p and the coefficient of friction μ ($\tau = \mu\ p$). The coefficient of friction between the contact surfaces of neighbouring interlocking blocks is taken as 0.3 following previous studies [16,45].

2.3. Model validation

To validate the suitability and accuracy of the above numerical modelling method, it is used to model the compressive behavior of interlocking block prisms in the authors' previous study [19]. As illustrated in Fig. 2a, the specimen is composed of two full-sized interlocking blocks and two half blocks at both ends. The compressive load is applied using displacement-controlled loading method. The interlocking block prism is numerically modelled using the above method in Section 2.2. Both perfect contact and imperfect contact are considered to simulate block imperfections at the joints. There is no gap between blocks at the joint for the perfect model. For the imperfect model, gaps between blocks are modelled. Each surface imperfection height was measured using a height dial indicator (Fig. 2b), and the measured gap sizes are applied to the numerical model with imperfect contact as shown in Fig. 2c. An average gap width is 0.29 mm with a standard deviation of 0.16.

Fig. 3 compares the compressive force versus axial displacement curves from the laboratory test and the numerical simulations. As shown, in the laboratory test the force increases gradually with the imposed displacement because of seating effect. As gaps gradually close, the force increases quicker until reaching the peak load of 112.8 kN and

Table 1
Material properties of interlocking block.

Mass density (kg/m^3)	Elasticity		Plasticity				
	Initial Young's modulus, E_0 (GPa)	Poisson's ratio υ	Dilatation angle ψ (°)	Eccentricity	Biaxial stress ratio f_{bo}/f_{co}	K	Viscosity Parameter
2565	13.49	0.2	30	0.1	1.16	0.67	0.0001

Note: K is the ratio between the second stress invariant on the tensile meridian and compressive meridian at initial yield.

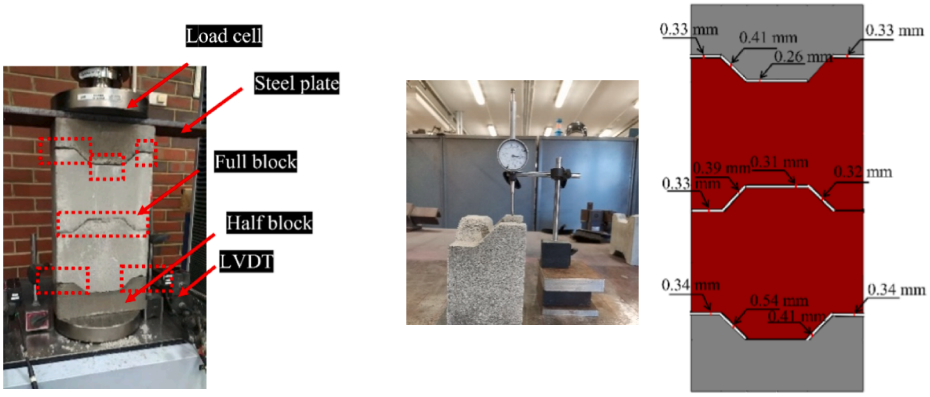

(a) experimental setup (b) measurement of imperfection (c) typical size of imperfection

Fig. 2. Experimental setup and numerical model.

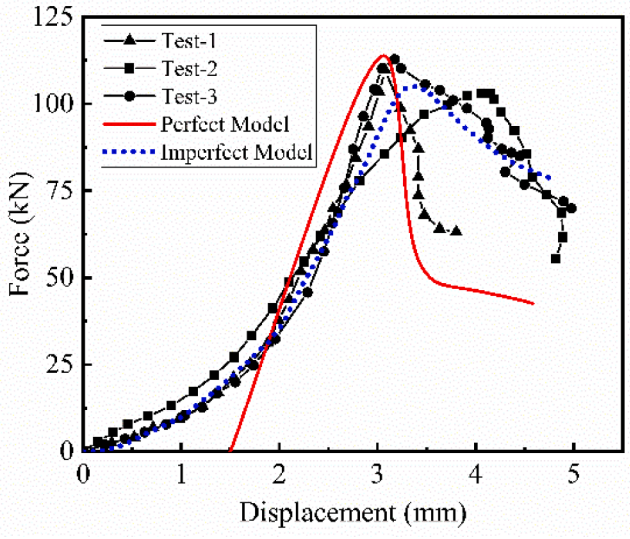

Fig. 3. Comparison of compressive force versus axial displacement curves from laboratory test and numerical modelling.

then plummets due to block damage. The numerical model with perfect contact predicts an ultimate load capacity of 113.8 kN. However, it could not model the seating effect because there are no pre-existing gaps. Moreover, an initial stiffness of 71.18 kN/mm is predicted, which is significantly larger than that of the lab test (61.85 kN/mm). The numerical model with imperfect contact predicts an ultimate capacity of 105.0 kN indicating less than 7% difference comparing to the lab testing result, while the predicted initial stiffness of 54.49 kN/mm by the numerical model with imperfect contact is much similar to that of the laboratory test.

It demonstrates that the numerical model considering block imperfection is crucial for proper estimation of the stiffness of mortarless interlocking block wall under compressive loading.

Fig. 4 compares the failure modes of interlocking block prisms from laboratory test and numerical simulations. In the laboratory test, wing cracks are initiated at the corner of the interlocking block key and extend both up and down. Due to the non-perfect contact conditions between neighbouring blocks, asymmetric failure mode is observed. The numerical model with imperfect contact predicts similar damage pattern where cracks initiate on the keys of the second block, and then extend vertically. The model with perfect contact predicts typical X-shaped failure because of the damages of shear keys due to symmetry, which could reflect the damage pattern of interlocking block but not able to fully represent the influence of imperfect blocks. Through the above comparison, it can be found that the developed numerical modelling

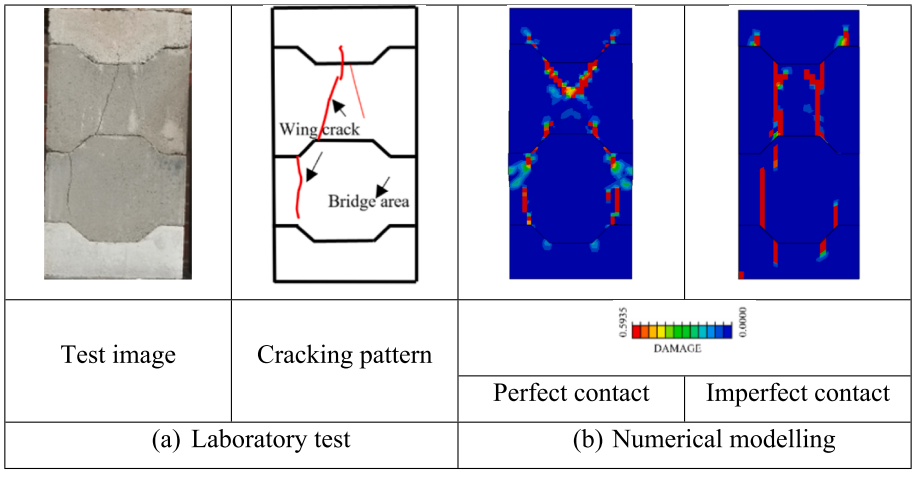

Fig. 4. Comparison of prism damage and failure patterns.

method could reasonably closely represent the behavior of mortarless interlocking block wall with consideration of block imperfection under compressive loading.

2.4. Size effect

The modelled wallet size (height 1200 mm, width 800 mm and thickness 100 mm) follows the recommendation of BS1052-1 [46] for the determination of compressive strength of the interlocking block wall. To examine the potential size effect and to quantify its influence on the modelled compressive strength of the mortar-less interlocking block wall, a group of masonry walls with different dimensions are numerically modelled, i.e. 600 mm × 400 mm × 100 mm, 1200 mm × 800 mm × 100 mm, and 2400 mm × 1600 mm × 100 mm (as shown in Fig. 5a). For easy engineering application, axial stress and strain are used to quantify the performance of the interlocking block wall in lieu of axial compressive load and displacement. The axial stress is the averaged compressive stress in the cross section which is calculated by dividing the measured axial compressive load by the cross-sectional area of the interlocking block wall; and the strain is calculated by dividing the vertical displacement with the initial height of the interlocking block wall. Fig. 5b compares the maximum compressive strengths and the initial stiffness, from which it can be found that varying the width and height of the wall model by four times leads to a maximum variation in the compressive strength by 3.40%, and a maximum variation in the stiffness by 0.23%. It demonstrates that the influence of model size on the compressive loading capacity is insignificant and the recommended wallet dimension by BS1052-1 is appropriate for predicting the compressive strength of mortar-less interlocking block wall.

3. Probabilistic models

Compared to conventional masonry where mortar bonds blocks together leading to negligible influence of block imperfection, dry-stacked interlocking blocks are constructed without mortar. Unavoidable imperfections in block could potentially result in significant local stress concentration and relative movements of adjacent blocks and thus influence the mechanical performance of the masonry structure. This paper focuses on quantifying the influence of geometric imperfections on the compressive properties of interlocking block walls, where other uncertainties such as block material strength, are not explicitly investigated. To study the influence of random imperfection of interlocking block on the compressive strength and axial stiffness of the interlocking block wall, the above-selected 1200 mm × 800 mm × 100 mm interlocking block wall with spatial block/joint imperfection is modelled.

3.1. Block and joint imperfection

Considering the manufacturing process of interlocking blocks which are pressed in mould using servo-controlled high-pressurized block machine, imperfections could occur to the produced blocks with variation to block heights, i.e., total block height, and shear key height, and inclined surfaces as shown in Fig. 1. Fig. 6 shows the set-up of interlocking block wall with spatial imperfections. Because of the asymmetric shear key layout on each interlocking block unit, the wide shear key and the small keys on the frontal and rear surfaces are shown respectively in Fig. 6a and Fig. 6b. Considering the shape and geometry of the shear keys, imperfections could exist on the flat surfaces or the inclined surfaces of the shear keys, as seen in Fig. 6c and 6d. It is to note that height imperfections on the flat surfaces are most common. This is because during the manufacturing process of the interlocking blocks, the weight of the material added into the mould and the pressure applied to compress the material remain constant for each block. However, due to variations in the moisture content of the block material, the height of the produced blocks may vary slightly, resulting in imperfections on the flat surface.

As shown in Fig. 6c, the imperfection height h means the roughness height normal to the surface of interlocking block. It is to note that the sizes of the above imperfections are normally small, since blocks with large imperfections will be filtered out in the quality control process, and blocks with large imperfections caused during transportation will also be identified in construction and usually discarded because they will not stack properly.

3.2. Stochastic analysis with Monte-Carlo simulation

The spatial variability of imperfection for interlocking block wall is generated using the above-mentioned numerical method in stochastic analysis based on the Monte-Carlo simulations. Since blocks are manufactured in large quantities, binominal distribution is employed to describe the existence of imperfection on each block unit. The probability of imperfection for the binominal distribution, p, depends on the quality control in block manufacture. Following the recommendation of block manufacturer, the probability of imperfection existence during manufacturing is stratified into four groups: high quality, high-medium quality, medium–low quality, and low quality, which correspond to 0–25%, 25–50%, 50–75%, and 75–100% possibility of each block unit having imperfections. p is assumed to follow uniform distribution within each group. It is worth noting that Monte-Carlo simulations usually use simple random sampling, which entails a large number of simulations to achieve convergence, therefore is computationally costly. The employed stratified sampling method could help to achieve an improved convergence rate. The stratified sampling method is operated by subdividing the sample space into smaller regions and sampling within these regions. In so doing, the produced samples could more effectively fill the sample space and therefore reduce the variance of computed statistical estimators. Previous study demonstrated this sampling method could provide fast converging analysis for Monte-Carlo simulation with

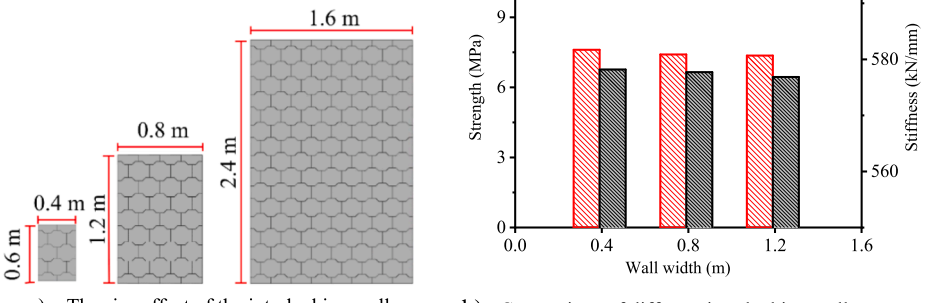

a) The size effect of the interlocking wall

b) Comparison of different interlocking walls

Fig. 5. Influences of size effect.

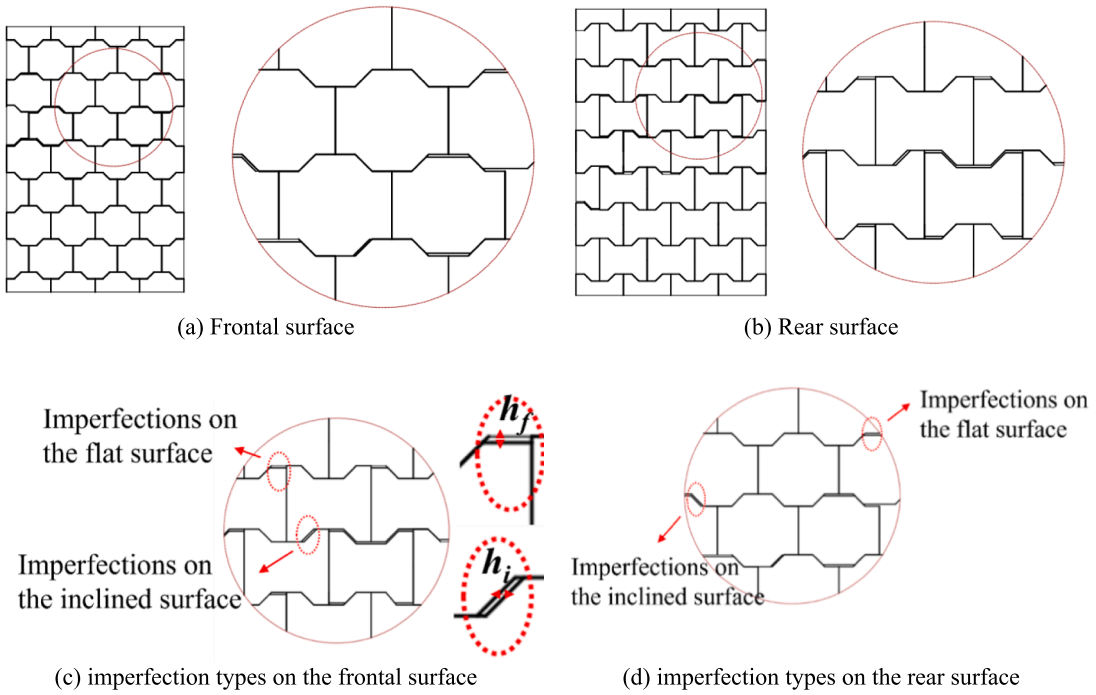

Fig. 6. Illustration of interlocking wall with random spatial imperfections.

satisfactory accuracy [47]. The imperfection size of each block unit is simulated following the truncated normal distribution with a mean of 0.3 mm, which was determined through statistical analysis on the different batches of block specimens [43]. The truncated normal distribution rather than the normal distribution is used herein to avoid a negative joint gap value. A python-based program is written to automatically generate interlocking block wall models in batches in Abaqus. Despite the complex configuration of blocks due to the random imperfections, in the numerical modelling all the initial locations of the blocks are set at the proper positions as an intact wall without considering the imperfection. The generation of spatial variability model can be expressed as follows:

(1) For a 1200 mm × 800 mm × 100 mm interlocking block wall, it comprises of 40 blocks (as shown in Fig. 7). Each block is labelled with a number from 1 to 40 in the sequence from the bottom left to the top right in layers.
(2) Depending on the location of the imperfections in one block, the imperfections of a block are classified into four types, i.e., height imperfection on the small keys, height imperfection on the large keys, slide (side) imperfection on the front sliding surfaces, and slide imperfection on the rear sliding surfaces. The existence of imperfection is randomly determined following the Binominal distribution with a possibility of p. The block quality is classified into four groups, i.e. high quality, high-medium quality, medium–low quality, and low quality, depending on the value of p.
(3) Once the location of imperfection in a block is determined, the imperfection size on the surface of this block is assumed to be uniform over the entire surface for simplicity. The imperfection size follows the truncated normal probability distribution with a mean $h_m = 0.3$ mm and a specific standard deviation. The characteristic value of imperfection height is estimated using $h = h_{\mathrm{m}} \pm 1.645\sigma$. Since there is very limited data on the standard deviation of imperfection size σ, the COV is assumed to vary between 0.1 and 0.5 [48].
(4) Each numerical model is established with the random spatial imperfection distribution, after which numerical modelling is carried out by loading the wall using displacement-controlled compression method till the failure of the wall. The peak compressive force and stiffness of the wall are determined through the axial load versus axial displacement curve simulated by the numerical analysis. The compressive strength of the interlocking block wall is determined with the peak compressive force.
(5) Convergence analysis is performed, where the accumulated mean compressive stress and accumulated compressive stress COV for the interlocking wall with different numbers of simulations are examined to determine the termination of numerical simulations. Repeat the above steps 1 to 4 until the statistical convergence is reached, in which the COV varies between 0.1 and 0.5. A COV of 0.1 represents the imperfection size has slight dispersion, while a COV of 0.5 represents the imperfection size has large dispersion.
(6) The average compressive stress is calculated by the ratio of the total force on the interlocking wall and the total sectional area of the block wall. The average strain is measured by the ratio of the compressed displacement at the top surface of the interlocking wall and the height of the interlocking wall. The data are counted into different groups with different COVs and/or different range of defect rates (p) and then used for construction of the histograms of compressive strength, equivalent stiffness and linear stiffness. The probability density function is generated and compared with specific probability density functions to determine the type of distribution.

3.3. Convergence study

Convergence test of Monte-Carlo simulations is performed with the numerical model for interlocking block walls of different qualities. Fig. 8 presents the variations of the mean compressive strength of interlocking block walls and its corresponding COV acquired from the Monte-Carlo simulations. It is found that after 60 random cases, the variations on the mean compressive strength and the corresponding COV are very small, indicating the simulations converge. Therefore, 60 simulations are needed to achieve the converged results. It is to note that the number of simulations to achieve convergence is small because the stratified sampling method is employed, which helps to unconditionally reduce

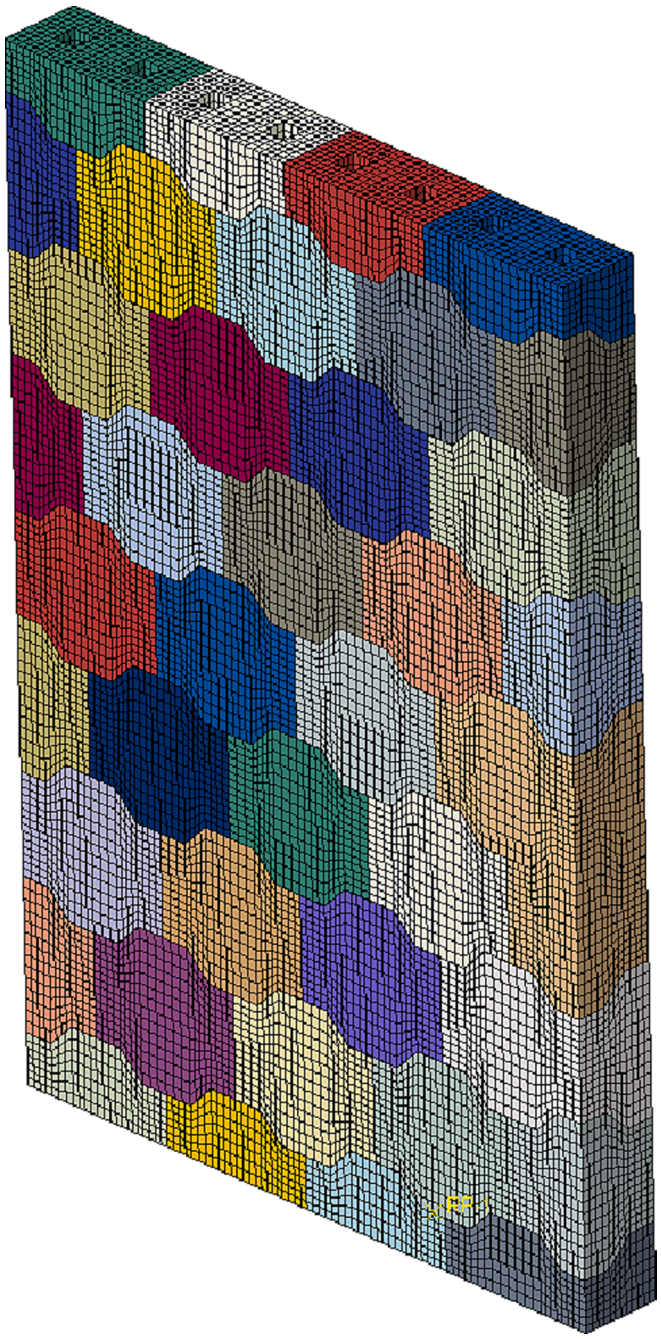

Fig. 7. Numerical model for the interlocking block wall.

the variance of statistical estimators when compared with the simple random sampling method [47].

4. Crack development and failure mode

Imperfection could influence the crack pattern of individual interlocking block unit, whose spatial distribution then influence the crack development and failure mode of the interlocking block wall. In this section, the crack pattern of individual interlocking block units with imperfections on different key surfaces are presented. Then, crack initiation and development of walls made of imperfect interlocking blocks are presented and analysed. The failure modes of the interlocking block wall with spatial distributed imperfections are discussed.

4.1. Cracking pattern

These imperfections could cause interlocking blocks to not fit tightly together at local vertical positions. Consequently, when the interlocking block wall is subjected to compression, the vertical stress is not uniformly distributed across the cross-section with stress concentrations at those contact points, which leads to premature failure of those blocks and ultimately affect the overall performance of the structure. Moreover, such non-uniform stress distribution could result in eccentric loading on the interlocking block structure and even cause out-of-plane buckling. Fig. 9 presents typical block cracking patterns caused by different types of block imperfections. One single interlocking block is modelled with its bottom fixed, and compressive load is applied gradually to its top until failure. Imperfection is introduced to different surfaces of this interlocking block to examine the associated crack patterns of the unit block. It is to note that there are more than dozens of combinations of imperfections on the different surfaces of an interlocking block, which nevertheless yield similar block cracking pattern. Therefore, only typical cases of block unit with imperfect surfaces are listed herein with unique cracking patterns. For Case 1, imperfection exists on the tenons of the rear surface (green highlighted area) while the other surfaces are all intact. With block imperfections, load can only be transferred through the contacting surfaces. As a result, two vertical cracks are initiated propagated downwards on the rear surface because of the increased stress owing to smaller contact area. When more imperfections exist on the rear surface as well as the frontal surface as in Case 2, cracks also initiate on the frontal surfaces. Moreover, because of unsymmetric imperfection on the inclined surfaces, unsymmetric damages can be seen on the block. In Case 3, imperfections exist on the inclined surfaces on the front key as well as the flat surfaces of the rear shear keys. Because of the unsymmetric load distribution on the block, crack initiates on the right wing of the rear surface.

With more imperfections existing on more surfaces of an interlocking block as in Case 4 where only the flat surfaces on the front shear key and one single surface on a rear key are intact, the applied compressive load can only be transferred through very limited regions in the block. As a result, crack is developed on the edge of the load-bearing surfaces and extends from the front of the block to the rear side of the block. In Case 5, the flat surfaces on the right wing of the front face are intact, through which load is transferred. Under gradually increased compressive load, crack is developed on this wing. Because of partial contact on the rear face of the block, this crack extends towards the rear surface of the block leading to the eventual failure.

From the above illustrations it can be seen that the existence of imperfection on dry-stacked interlocking block on different surfaces could strongly influence the cracking pattern. Those imperfections, which determines the load transfer path in one single block, would interact with adjacent blocks when multiple blocks are stacked together to create an interlocking block wall. The crack development and failure mode of interlocking block walls with different quantity of imperfections, their spatial distributions and different imperfection sizes would therefore be different, which will be analyzed and discussed in the following section.

4.2. Initial crack and crack development in a wall

To demonstrate crack development and wall failure mode of interlocking block walls with spatially varying imperfections, without loss of generality four typical interlocking block walls made of high-quality, high-medium quality, medium–low quality and low-quality blocks are analysed. Fig. 10a shows the load path, damage/crack patterns. The randomly generated imperfection locations and sizes are highlighted in green colour (darker indicates larger imperfection size). The corresponding load–displacement curves are shown in Fig. 10b. For the high-quality wall, the compressive load increases almost linearly with the axial displacement of the wall until Point A (more than 75% of

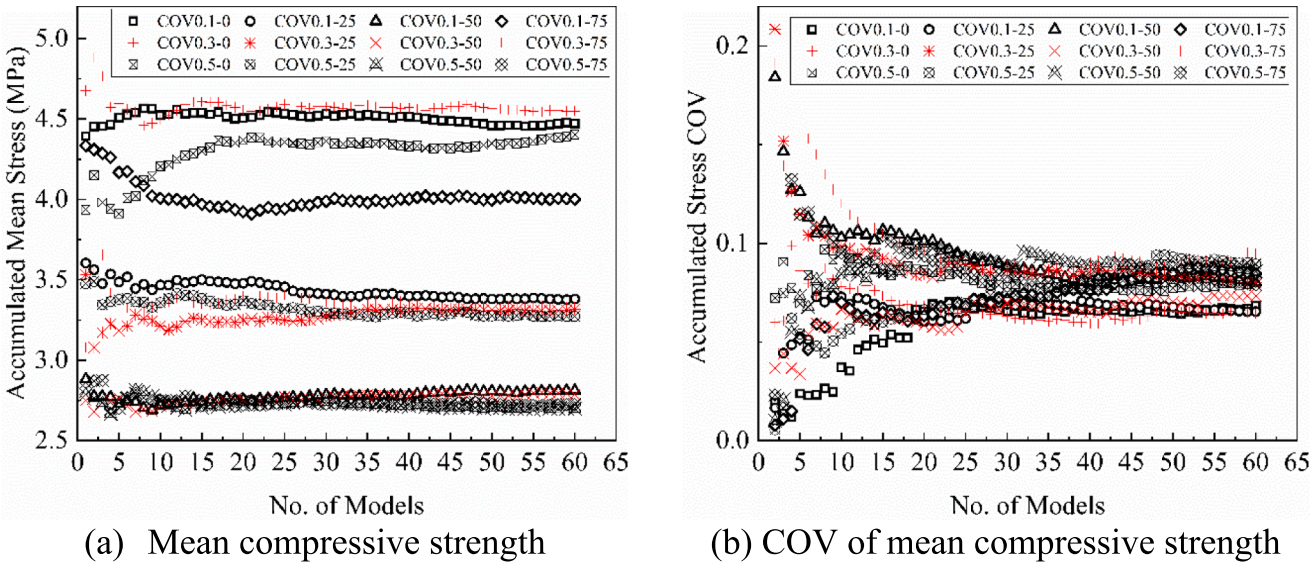

Fig. 8. Convergence of Monte-Carlo simulations.

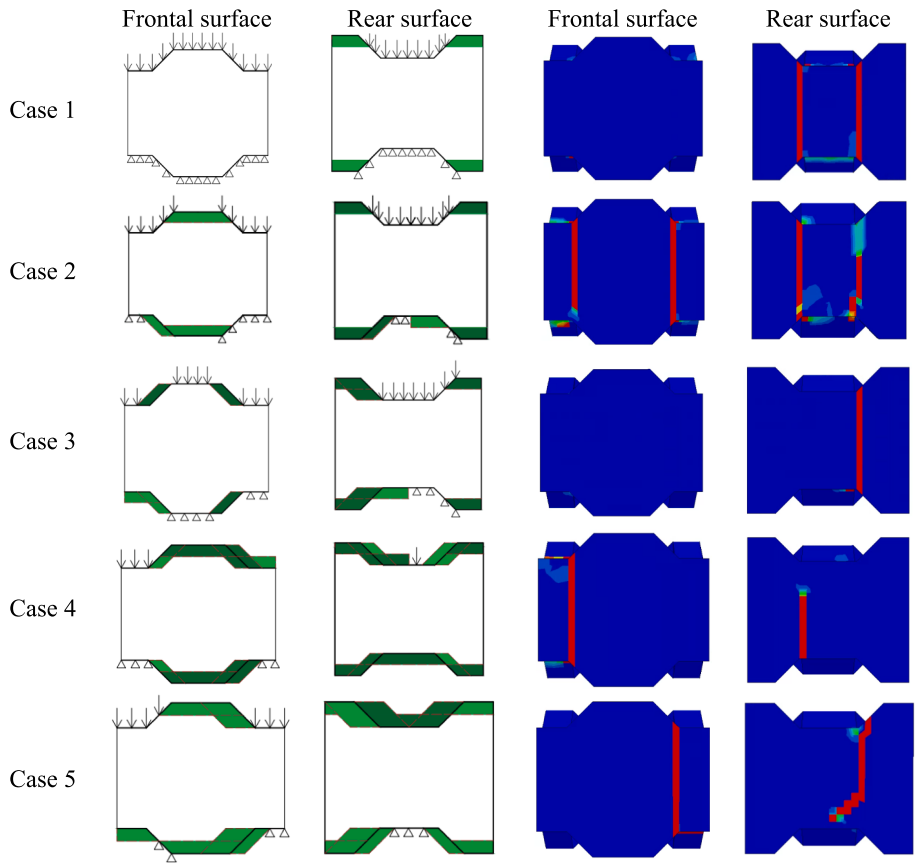

Fig. 9. Crack patterns for interlocking block with different imperfections.

compressive strength is achieved), when crack initiates on the wall. As can be seen in Fig. 10a, initial cracks are developed on the interlocking blocks with large size imperfections. This is because under compressive loading, smaller joint gaps due to block imperfections would close earlier than the larger gaps, which enables load transfer at these joints and hence more uniform stress distribution. But it also leads to non-uniform joint gaps with large block imperfections, which causes stress concentration and hence crack initiation. For the high-medium quality wall, the compressive load that the wall could withstand increases linearly to about half of the maximum compressive strength, which is lower than that of the high-quality interlocking wall. Being similar to the high-quality wall, cracks initiate around the joints with larger size imperfections. It can be seen from Fig. 10a that for the high-quality and high-medium quality wall, because relatively less imperfections exist and smaller imperfections would close under the imposed compressive loading first, the compressive force can then be transferred through

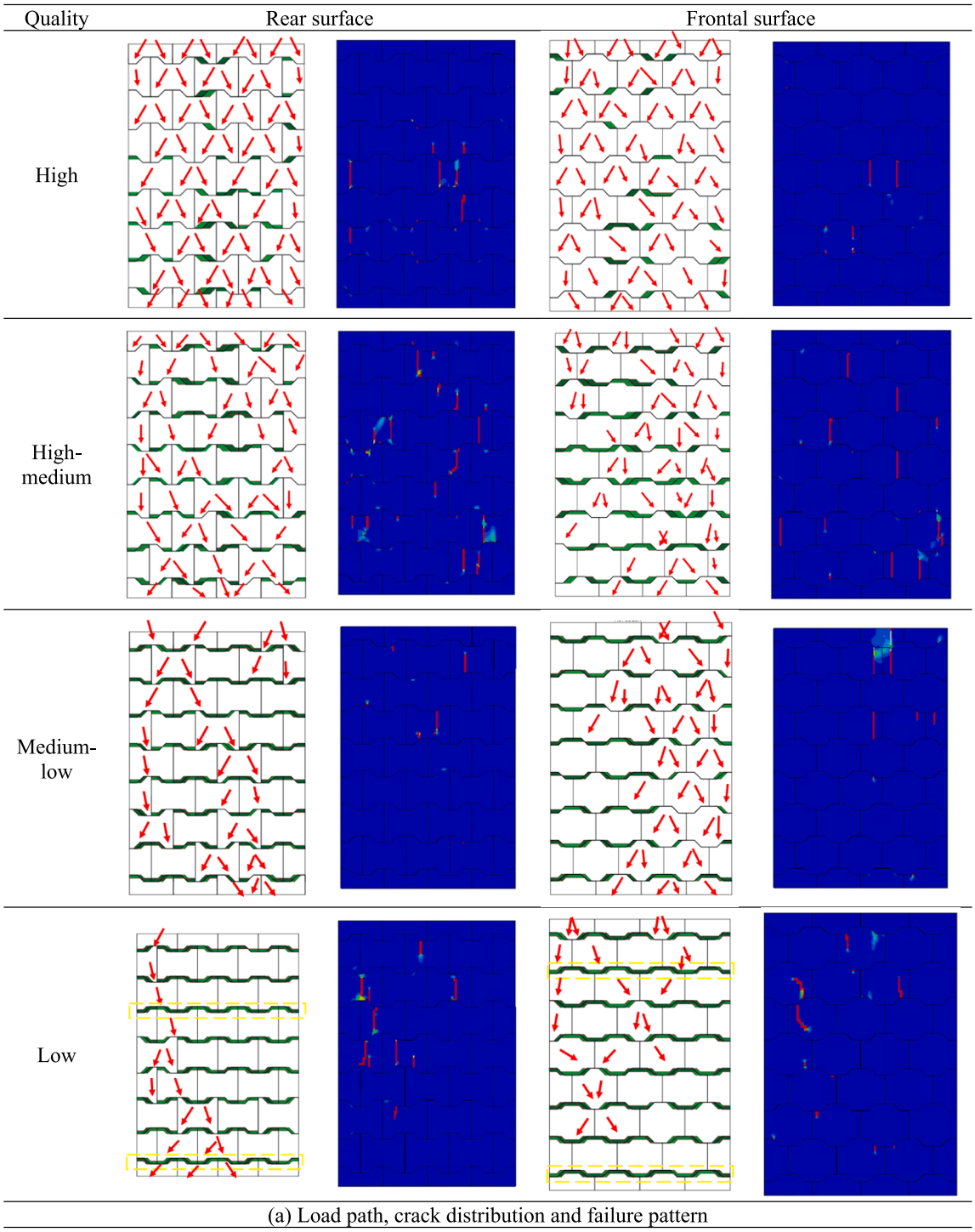

Fig. 10. Initial crack and load path at the stage of OA.

multiple load paths over the interlocking blocks. For the low-quality wall, because of the widely spread imperfections on blocks, under the initial compressive loading, less contacts are developed between blocks resulting in seating effect (as highlighted in yellow). As a result, with the increased compressive loading, only less number of load paths are developed. Similar to the medium–low quality wall, initial cracks are developed around the load path where blocks are bearing high compressive stress. As shown, the low-quality block wall has higher compressive strength than the medium–low and high-medium quality wall although its equivalent stiffness is small owing to a relatively large initial seating movement to close the gap between blocks. This is because the low quality wall is associated with wider spread imperfections. Under compressive loading, the gaps in block wall close relative uniformly, whereas the medium–low and high-medium quality walls have less number of imperfections. Under compressive loading, closing of the gaps is not uniform and causes stress concentration, hence more damage to the blocks. Therefore, their compressive loading capacity is smaller than that of the low-quality wall.

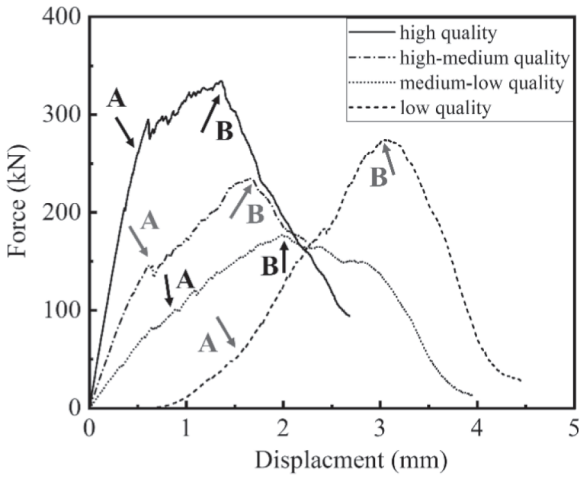

(b) Force-displacement curves

Fig. 10. (*continued*).

4.3. Failure mode

As the imposed compressive load continues to increase, these cracks extend, and more cracks are developed until the maximum compressive strengths of each wall are reached. Fig. 11 shows the eventual damage contours of the four interlocking block walls of different qualities. Because the distribution and size of block imperfections are random, the crack pattern are asymmetric and random. Block cracks widely spread among the walls. But some common cracking similarities exist in these four quality interlocking walls. Cracks initiate from the shear keys with vertical cracks indicating tensile damage [19]. Compressive damages are then developed in the cracked blocks as the wall is subjected to further increased compressive loading. It indicates that increasing the post-cracking strength of interlocking blocks would improve the mechanical performance of interlocking block wall under compressive loading. In the meanwhile, some differences can be observed on these four different quality interlocking block walls: for the high-quality and high-medium quality walls, since the majority of blocks are intact thus in full contact for the compressive load to transfer through, the load distributes relatively uniformly and thus cracks are also more uniform, which leads to a higher compressive capacity and stiffness than those of the walls of the other qualities. For the medium–low quality wall with more imperfected blocks, load is redistributed after the initial cracking of blocks around the load path. More blocks are thus to bear the compressive force. More cracks can be observed on the failed walls when the peak compressive capacity of the wall is reached. For the low-quality wall with the majority of blocks having imperfections, joint openings due to block imperfection actually would close under the initial compressive loading, leading to a more uniform distribution of stress on the entire block wall. As a result, on the final damage contour of the low-quality wall, cracks are distributed widely and more uniformly as compared with the medium–low quality wall.

5. Results and analysis

The influence of random imperfections of interlocking blocks on the compressive behavior of interlocking block wall is presented and analysed in this section. The compressive stress–strain curves are firstly presented. The compressive strength and axial stiffness of interlocking block wall are summarized and analysed.

5.1. Stress–strain curves

Fig. 12 displays the compressive stress–strain curves for interlocking block walls with varying quality and imperfections. Engineering stress and strain are used, which are calculated based on the net cross section area and the wall height, respectively, offering a clear visual on how the strength and deformability of the wall are affected by imperfections.

The stress–strain curves for high to low-quality walls, with a coefficient of variation (COV) of 0.1, reveal significant differences. High-quality walls exhibit a linear elastic behaviour up to 75% of the maximum compressive capacity, followed by a non-linear increase and an eventual decrease, indicative of considerable damage. High-medium quality walls demonstrate a similar pattern, but the linear elastic stage is shorter, only lasting to about 50% of compressive capacity. This is because in the high-medium quality wall, there are more imperfections, resulting in a smaller compressive stress distribution area and a more uneven distribution pattern on the cross-section of the wall. This, in turn, leads to the earlier arrival of the elastoplastic stage in the high-medium quality wall. As block quality deteriorates, the influence of block imperfection variation on the initial modulus becomes increasingly evident due to the larger number of imperfections. For low-quality walls, pronounced seating effects are observed in their stress–strain curves, which is a result of the gradual closure of the gaps due to imperfections under compressive loading.

While the compressive strength of the wall decreases as the block quality lowers from high to high-medium and then to medium–low, an increase is observed in the walls with low-quality blocks compared to the walls with medium–low quality blocks despite a considerable decrease in initial equivalent stiffness when the COV is 0.1 and 0.3. This counterintuitive result can be attributed to the relatively uniform imperfection distribution in those low-quality blocks with a relatively small imperfection variation, causing an apparent seating effect, i.e., initial slippage at low compressive load. Upon the closure of imperfection gaps caused by compression, a near-linear behaviour similar to high-quality walls is observed due to the increased contact area between blocks, suggesting that uniform imperfection distribution can compensate for the lack of block quality to some extent.

In summary, the probability of block imperfection negatively impacts wall quality and initial compressive stiffness, particularly for the first three quality levels. However, for low-quality blocks with relatively low block imperfection variation, as gaps close after the strong seating effect, the wall behaves similarly to a high-quality block wall. Thus, the

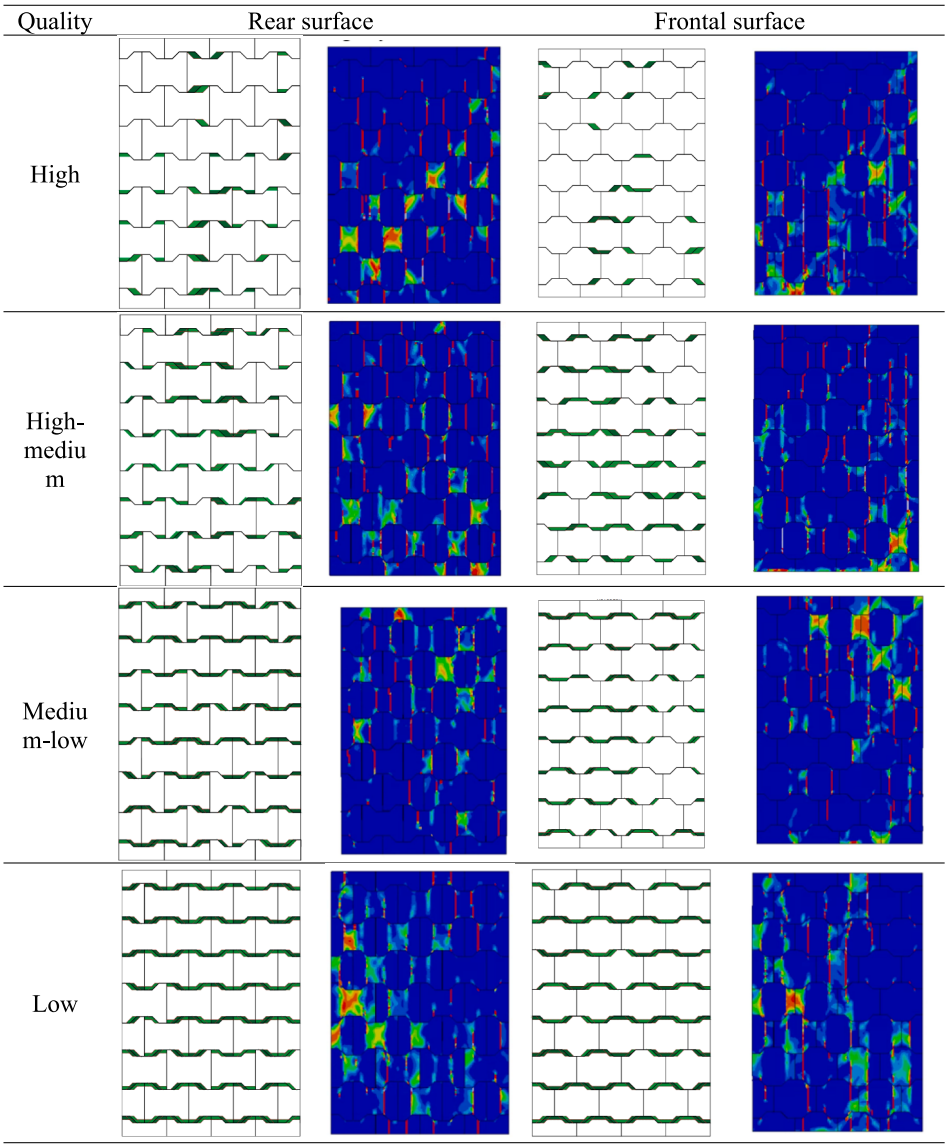

Fig. 11. Damage contours of interlocking block wall at peak compressive loads.

distribution of block imperfections plays a significant role in determining the compressive strength and deformability of interlocking block walls.

5.2. Compressive strength and probability distribution

The compressive strengths derived from the stress–strain curves for the interlocking block walls with varying quality and imperfections are summarized in Table 2. The table lists mean compressive strength, standard deviation σ, and the associated coefficient of variation (COV_f) for each quality category. Fig. 13 depicts the predicted compressive strength from the spatial analysis.

High-quality walls with fewer imperfect blocks exhibit the highest mean compressive strength. The COV of block imperfection sizes only slightly affects the mean compressive strengths of high and high-medium quality walls due to the limited number of block imperfections. However, for medium–low and low-quality walls, an increase in COV results in a decline in compressive strength, with low-quality walls seeing a significant drop from 4.00 MPa to 2.72 MPa as COV increases from 0.1 to 0.5. This is because in low-quality walls, most gaps close under compressive loading. A smaller COV results in more uniform gap closures and better inter-block contact and hence leads to relatively high compressive strength. Conversely, a larger COV, indicating non-uniform imperfection distributions, can result in more local damage due to stress concentrations, thereby reducing the wall's compressive loading capacity.

Fig. 14 presents the histograms of wall compressive strengths, which are modeled using different probability distribution functions. These histograms demonstrate that the increase of COV of imperfection size scatters the compressive strength of the interlocking block wall, with a heavier tail for COV = 0.5, indicating a greater probability of wall failure before reaching the predicted compressive strength. Particularly for low-quality walls, an increase in COV significantly reduces the wall strength, as explained above.

In summary, these results highlight the role of COV in block imperfections in determining wall compressive strength, suggesting that neglecting this factor may overestimate the compressive capacity, especially for low-quality walls.

5.3. Equivalent stiffness and probability distribution

To quantify wall stiffness, the equivalent stiffness is introduced, defined as the slope of the secant line from the origin to the peak compressive force on the modelled stress–strain curves (Fig. 15). Fig. 16

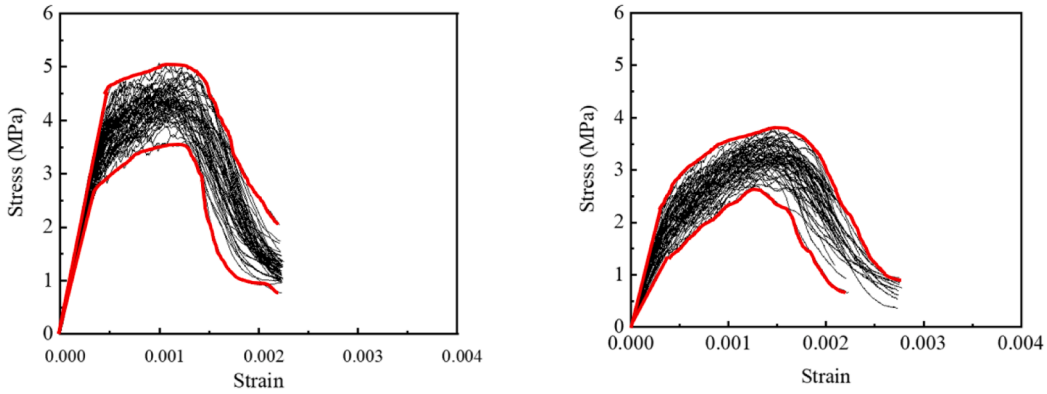

(a) High quality wall with COV=0.1

(b) High-medium quality wall with COV=0.1

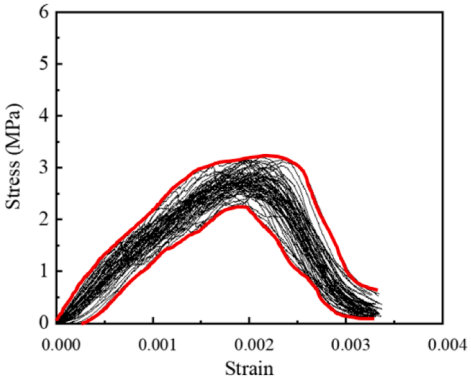

(c) Medium-low quality wall with COV=0.1

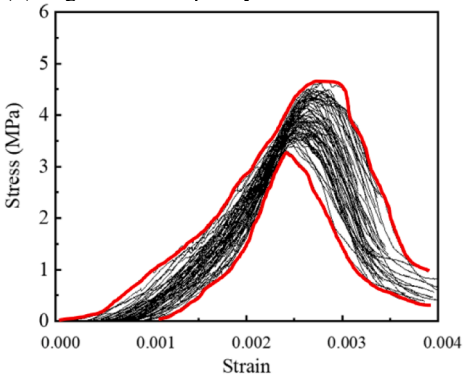

(d) Low quality wall with COV=0.1

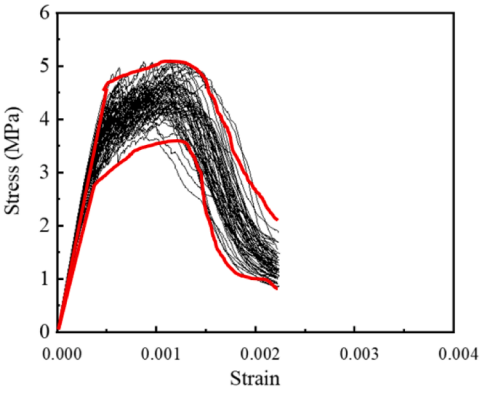

(e) High quality wall with COV=0.3

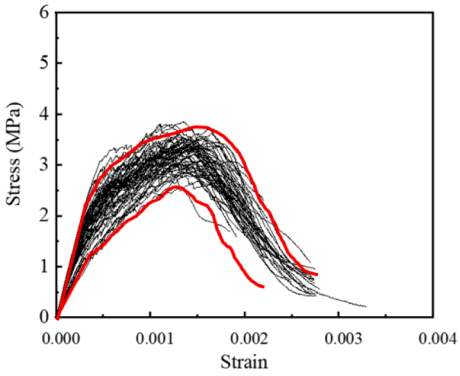

(f) High-medium quality wall with COV=0.3

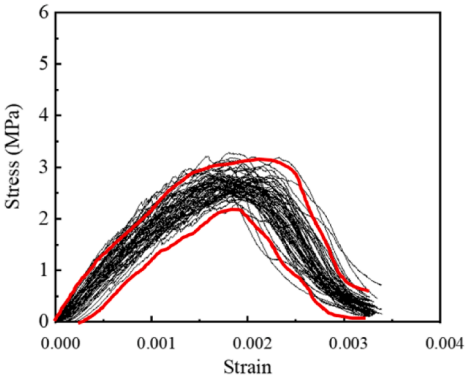

(g) Medium-low quality wall with COV=0.3

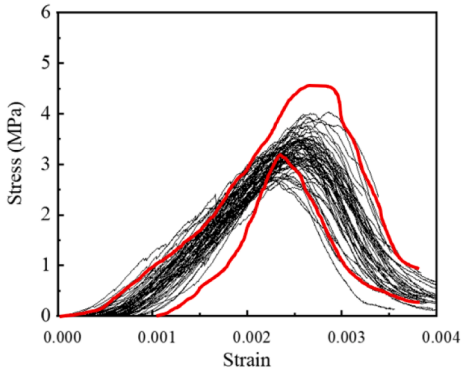

(h) Low quality wall with COV=0.3

Fig. 12. Stress–strain curves of interlocking block walls with spatially varying imperfections.

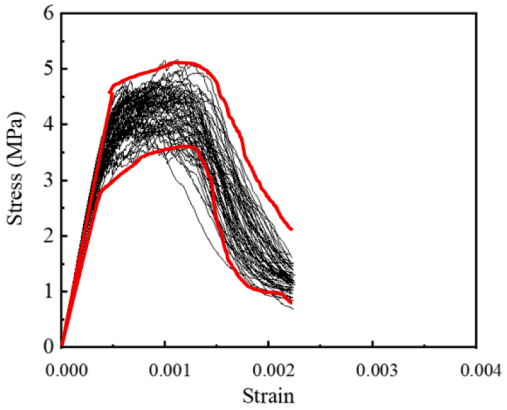

(i) High quality wall with COV=0.5

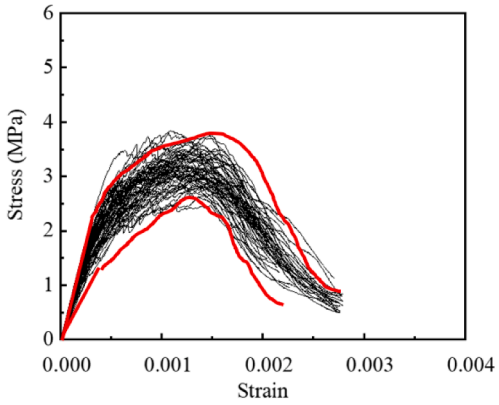

(j) High-medium quality wall with COV=0.5

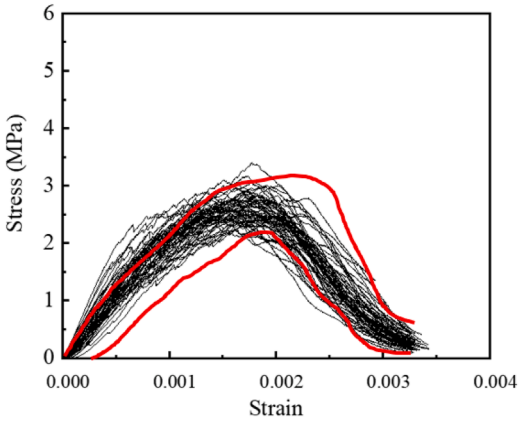

(k) Medium-low quality wall with COV=0.5

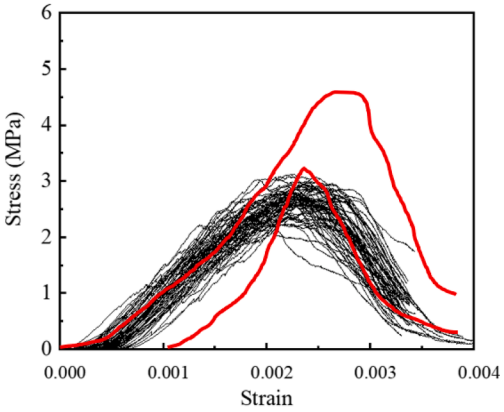

(l) Low quality wall with COV=0.5

Fig. 12. (*continued*).

Table 2
Summary of wall compressive strengths from Monte-Carlo analysis.

Imperfection	High-quality wall						High-medium quality wall					
COV	$f_{Max.}$ (MPa)	f_{Min} (MPa)	f_{Mean} (MPa)	σ (MPa)	COV_f	Distribution	$f_{Max.}$ (MPa)	$f_{Min.}$ (MPa)	f_{Mean} (MPa)	σ (MPa)	COV_f	Distribution
0.1	4.96	3.94	4.47	0.26	0.058	Normal	2.83	3.84	3.38	0.22	0.065	Loglogistic
0.3	5.12	3.88	4.55	0.29	0.064	Loglogistic	3.86	2.63	3.32	0.27	0.080	Weibull
0.5	5.17	3.64	4.40	0.36	0.081	Normal	2.47	3.84	3.27	0.29	0.090	Normal
Imperfection	Medium-low quality wall						Low-quality wall					
COV	$f_{Max.}$ (MPa)	$f_{Min.}$ (MPa)	f_{Mean} (MPa)	σ (MPa)	COV_f	Distribution	$f_{Max.}$ (MPa)	$f_{Min.}$ (MPa)	f_{Mean} (MPa)	σ (MPa)	COV_f	Distribution
0.1	3.16	2.44	2.81	0.18	0.060	Normal	4.65	3.36	4.00	0.34	0.085	Normal
0.3	3.28	2.36	2.79	0.20	0.070	Loglogistic	4.04	2.70	3.33	0.32	0.095	Gamma
0.5	3.41	2.17	2.70	0.23	0.086	Loglogistic	3.12	2.17	2.72	0.22	0.079	Smallest Extreme

and Table 3 illustrate the distributions and statistics of equivalent stiffness for different imperfection size COVs.

As expected, the mean equivalent stiffness decreases with increasing imperfection quantity, attributable to a corresponding increase in peak compressive load displacement. This highlights the potential for overestimation of dry-stacked block wall stiffness in numerical models neglecting existing imperfections [16,19].

Interestingly, as COV increases from 0.1 to 0.5, the equivalent stiffness of high-quality, high-medium-quality and medium–low-quality walls increases. This counterintuitive result could be due to significant decreases in peak load displacements despite minor variations in peak compressive load. With a wider and non-uniform distribution of block imperfections in the wall, local damage from stress concentration will occur, reducing the wall displacement at failure. Conversely, low-quality walls exhibit a decrease in equivalent stiffness with increasing COV, which is a result of the significant drop of the wall's compressive strength with the increase of the COV of block imperfection sizes, as explained in Section 5.2.

These results underscore the strong influence of imperfection size distribution (COV) on the equivalent stiffness of interlocking block

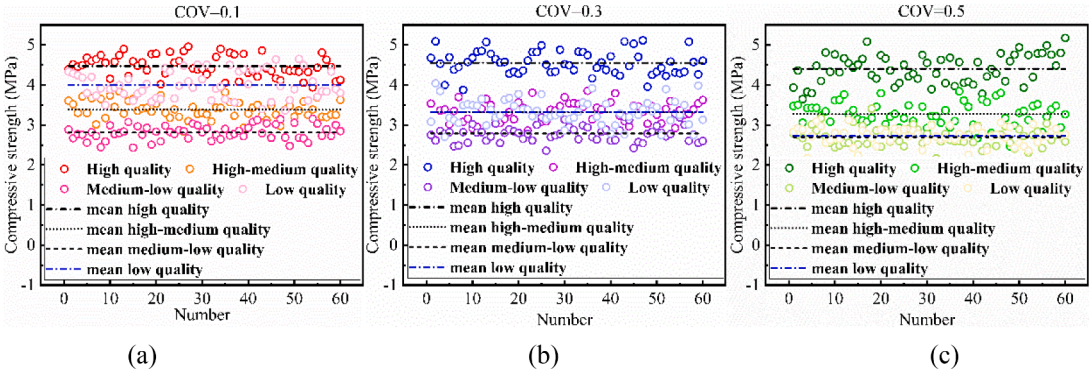

Fig. 13. Distribution of wall compressive strengths corresponding to different COVs of block imperfections.

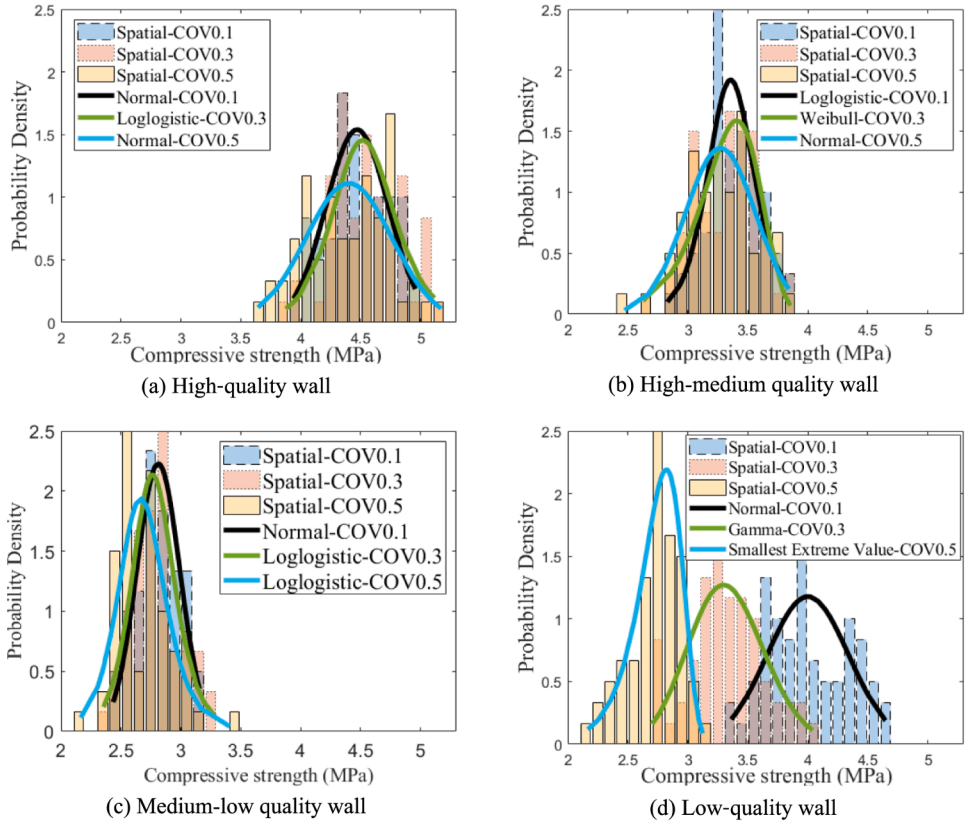

Fig. 14. Histograms of compressive strength for interlocking walls.

walls. It is noted that low-quality walls with COV = 0.1 have higher equivalent stiffness than medium–low quality walls. This is also due to the significantly higher compressive strength of low-quality walls with low COV of block imperfection sizes compared to that of the medium–low-quality walls.

Fig. 17 presents equivalent stiffness histograms and best-fit probability distribution functions, indicating a gradual dispersion of equivalent stiffness with increasing COV. For high-quality walls, there is a larger possibility of high equivalent stiffness with the increase of the COV of block imperfection sizes, while for low-quality walls, increasing COV significantly reduces the equivalent stiffness, which conform to the above analyses. It is noteworthy that the histograms for low-quality walls (Fig. 17d) are higher and narrower, which suggests less variability in equivalent stiffness compared to other walls of different qualities. This is a consequence of the simultaneous decrease in compressive strength and the corresponding displacement in low-quality walls as the COV of block imperfection sizes increases.

5.4. Linear stiffness and probability distribution

For high-quality and high-medium quality walls, where seating effect is negligible, the linear stiffness is defined as the slope of the secant line from the origin to the softening stage's starting point. For walls of medium–low and low-quality blocks, the seating effect is pronounced. Therefore, the linear stiffness is determined as the slope of the load–displacement curves' linear portion to reflect the wall's post-seating and prior-to-non-linear behavior.

As presented in Table 4 and Fig. 18, a correlation exists between the wall's quality and its linear stiffness. High quality, high-medium and medium–low quality walls have mean linear stiffness values of 511kN/mm, 320kN/mm, and 119kN/mm (COV = 0.1), respectively, implying that decreasing wall quality (i.e., increasing imperfections and reducing contact areas) significantly diminishes linear stiffness. The mean linear stiffness for these wall qualities sees a gradual increase as the COV of block imperfection sizes increases. The larger variation of imperfection

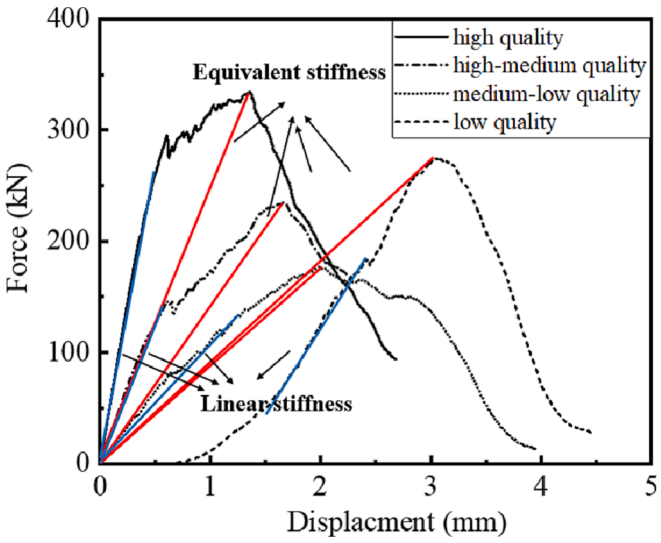

Fig. 15. The definition of equivalent stiffness and linear stiffness.

size allows some blocks to touch each other at lower displacements, leading to stress concentration at those contact points. Hence, the walls enter the elastic–plastic stage at lower displacements, causing the increase of the linear stiffness considering the relatively small change of compressive strength with the increase of the COV of imperfection sizes for these quality levels. This phenomenon, however, is not observed for low-quality walls, where increasing COV leads to a decrease in linear stiffness from 231kN/mm (COV = 0.1) to 113.5kN/mm (COV = 0.5). This can be attributed to the prevalent imperfections in low-quality walls that result in a significant seating effect. As COV = 0.1, most gaps close uniformly due to similar imperfection sizes, creating a larger contact area and, thus, a greater linear stiffness.

The histograms of linear stiffness (Fig. 19) indicate that for high-quality, high-medium quality, and medium–low quality walls, the distribution of linear stiffness remains relatively stable as COV increases. Conversely, the linear stiffness of low-quality walls becomes more scattered as COV decreases. An increase in the COV of imperfection size generally results in a decrease in linear stiffness and a narrower range of variation, whose reasons are explicated above. The findings underscore the significant influence of wall quality and imperfection distribution on the linear stiffness of interlocking block walls, particularly in low-quality walls.

6. Limitations and implications

The imperfections in the numerical model used in this study is based on the measurement data of blocks from a specific manufacturing machine. Since the block imperfection data could vary between machines and using different mixture recipe, the statistical data and analysis results could also vary. Nevertheless, the presented research method and the validated numerical model could find direct applications in future analysis and/or other type of dry-stacking interlocking block structures.

Despite the above limitations, the results of this study will find direct applications in the engineering design of interlocking brick structures and make the assessment of their compressive load-bearing capacity more accurate. Secondly, this study could help to evaluate the structural safety of dry-stacking interlocking block structure, thereby reducing the risk of potential failures. Last but not the least, the results of this study help to improve the quality control of brick manufacture, which demonstrate that the rigorous monitoring of imperfections during the brick production process is of utmost importance but consistency of quality and imperfection size could be more important. While low-

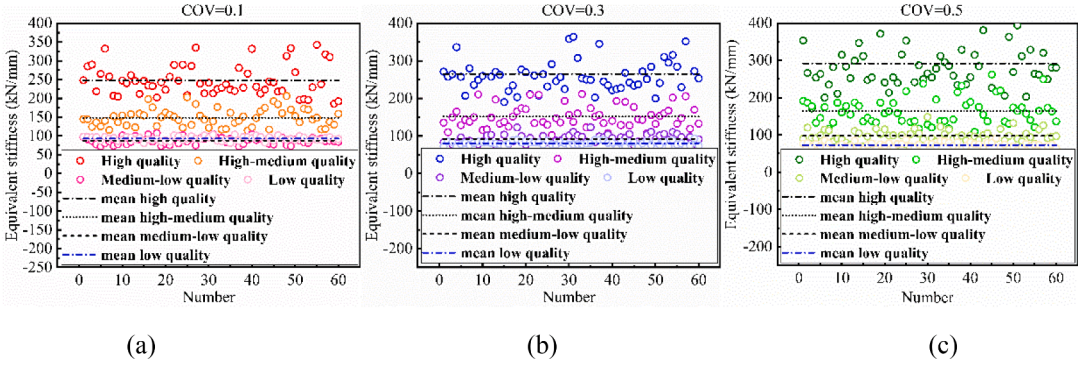

Fig. 16. Distribution of wall equivalent stiffness corresponding to the different COVs of block imperfection size distributions.

Table 3
Summary of wall equivalent compressive stiffness from Monte-Carlo analysis.

Imperfection	High-quality wall						High-medium quality wall					
COV	$E_{Max.}$ (kN/mm)	E_{Min} (kN/mm)	E_{Mean} (kN/mm)	σ (kN/mm)	COV_E	Distribution	$E_{Max.}$ (kN/mm)	$E_{Min.}$ (kN/mm)	E_{Mean} (kN/mm)	σ (kN/mm)	COV_E	Distribution
0.1	342.64	185.64	247.94	40.45	0.163	Loglogistic	206.20	114.20	148.31	23.30	0.157	Gamma
0.3	442.85	190.09	265.00	51.09	0.193	Loglogistic	211.30	101.80	151.70	28.68	0.189	Loglogistic
0.5	460.04	170.72	291.38	66.70	0.229	Loglogistic	262.00	108.30	163.77	35.10	0.214	Gamma
Imperfection	Medium-low quality wall						Low-quality wall					
COV	$E_{Max.}$ (kN/mm)	$E_{Min.}$ (kN/mm)	E_{Mean} (kN/mm)	σ (kN/mm)	COV_E	Distribution	$E_{Max.}$ (kN/mm)	$E_{Min.}$ (kN/mm)	E_{Mean} (kN/mm)	σ (kN/mm)	COV_E	Distribution
0.1	107.73	72.05	87.75	9.25	0.105	Normal	103.60	80.71	92.90	5.49	0.059	Normal
0.3	123.20	73.79	92.21	11.65	0.126	Loglogistic	93.34	67.43	80.47	5.76	0.072	Normal
0.5	147.86	68.49	97.68	15.39	0.16	Loglogistic	90.93	60.12	72.61	7.04	0.097	Normal

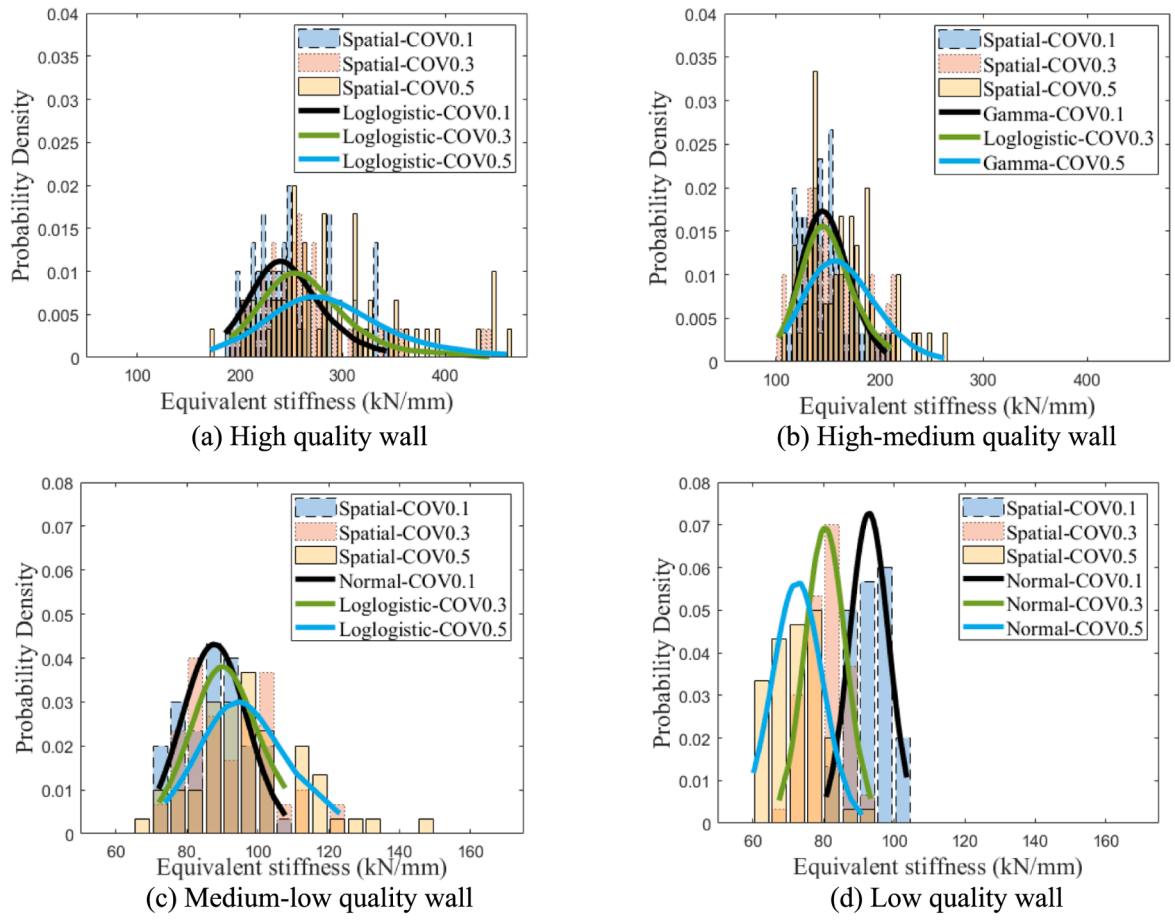

Fig. 17. Histograms of equivalent stiffness for interlocking block walls.

Table 4
Summary of wall linear stiffness from Monte-Carlo analysis.

Imperfection	High-quality wall						High-medium quality wall					
COV	$E_{Max.}$ (kN/mm)	E_{Min} (kN/mm)	E_{Mean} (kN/mm)	σ_E (kN/mm)	COV_E	Distribution	$E_{Max.}$ (kN/mm)	E_{Min} (kN/mm)	E_{Mean} (kN/mm)	σ_E (kN/mm)	COV_E	Distribution
0.1	575.04	439.63	511.44	28.34	0.055	Normal	439.79	212.16	320.30	48.57	0.152	Normal
0.3	590.62	439.95	521.99	29.75	0.057	Normal	415.77	216.33	324.09	49.42	0.153	Normal
0.5	604.49	474.61	533.24	30.11	0.056	Normal	418.84	258.70	334.76	40.41	0.121	Normal
Imperfection	Medium-low quality wall						Low-quality wall					
COV	$E_{Max.}$ (kN/mm)	E_{Min} (kN/mm)	E_{Mean} (kN/mm)	σ_E (kN/mm)	COV_E	Distribution	$E_{Max.}$ (kN/mm)	E_{Min} (kN/mm)	E_{Mean} (kN/mm)	σ_E (kN/mm)	COV_E	Distribution
0.1	158.78	79.97	119.35	19.59	0.164	Loglogistic	350	121.79	231.04	51.35	0.22	Lognormal
0.3	184.63	90.99	126.03	20.83	0.165	Loglogistic	181.37	93.85	132.87	20.24	0.15	Normal
0.5	217.41	104.82	148.51	24.66	0.166	Gamma	142.68	81.37	113.53	15.01	0.13	Normal

quality walls may even exhibit higher compressive strength than walls made of blocks with mixed qualities due to the more uniform compression of gaps if the imperfections are of similar sized, however, it would have significant seating effect even if the wall is subjected to relatively low compressive loading, causing the subsidence of the whole structure. More generally, the number and severity of localised block damage and failures increase with decreasing block quality, leading to a lower compressive strength and axial stiffness. This signifies that to maintain the structural performance and compressive load-bearing capacity of interlocking block walls, it is necessary to minimize the quantity of imperfect blocks and control the sizes of imperfections as much as possible during production.

7. Conclusion

This study performs stochastic analysis to investigate the compressive properties of dry-stacked interlocking block walls with spatially varying block imperfections. A detailed numerical model of interlocking block walls with block imperfection is generated. The number of block imperfections is assumed to follow the Binominal distribution in massive block production process. The imperfection sizes are assumed to follow the truncated normal distribution. the imperfection size on the surface of this block is assumed to be uniform over the entire surface for simplicity. The influences of imperfection on the compressive strength, equivalent stiffness, linear stiffness of interlocking block wall are studied. The following conclusions are derived from this study:

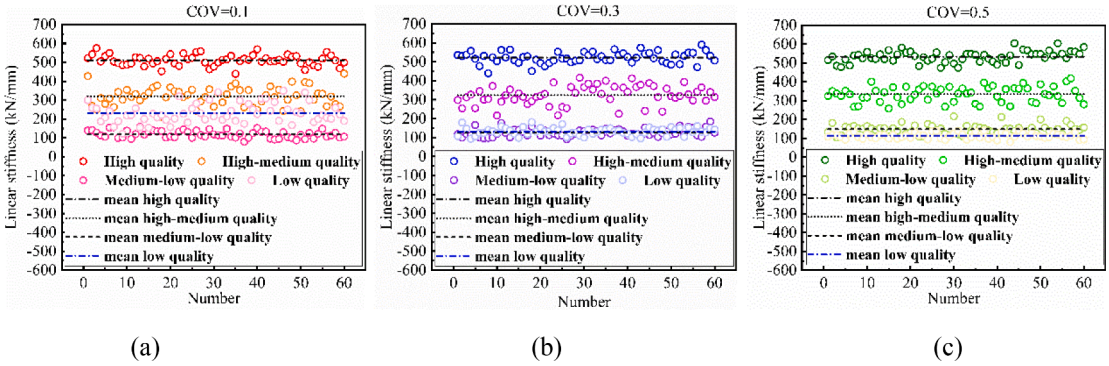

Fig. 18. Distribution of wall linear stiffness corresponding to different COVs of block imperfection size distributions.

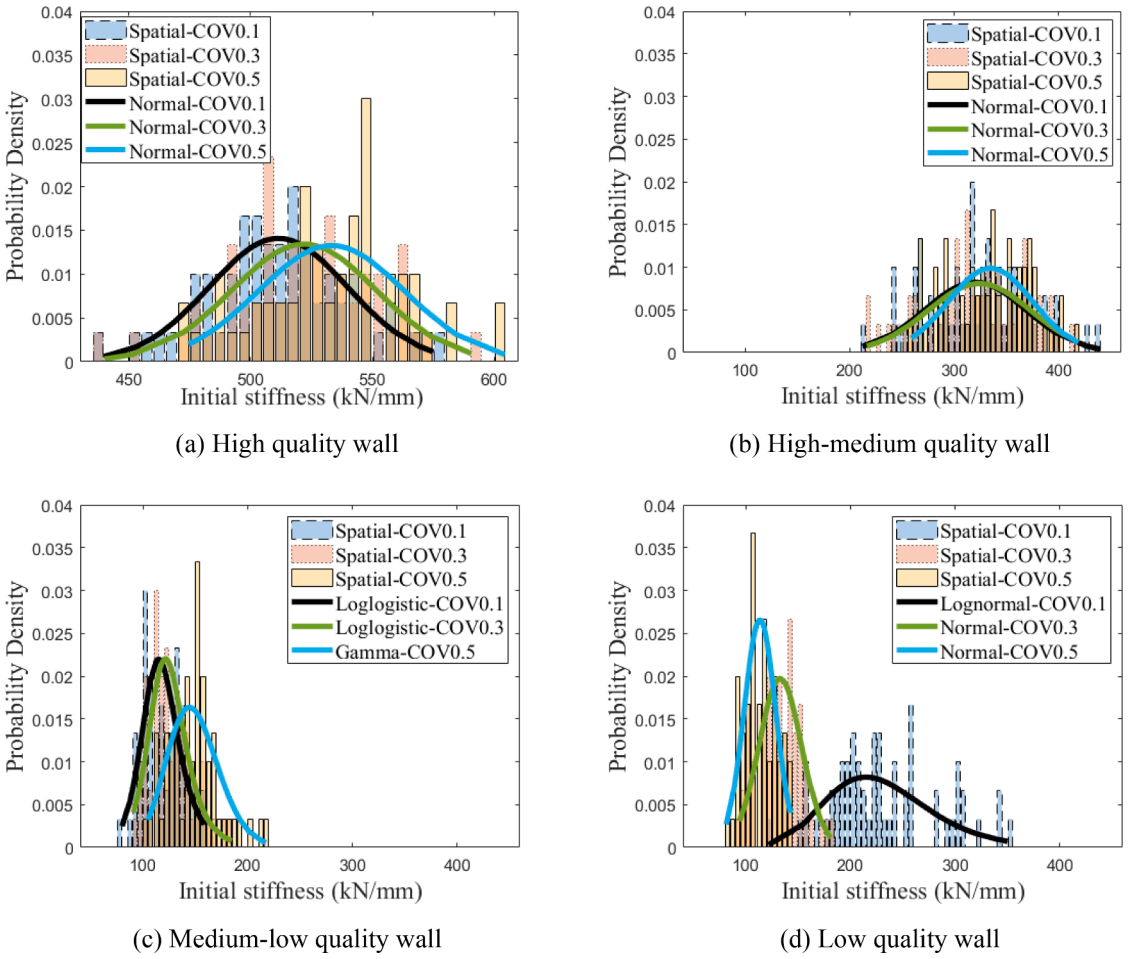

Fig. 19. Histograms of linear stiffness for interlocking walls.

1. Typical crack patterns on imperfect block units are presented, which demonstrates strong influence of imperfection on the crack patterns. It is also found that block imperfections could strongly influence the crack initiation and development, as well as the load path of dry-stacked interlocking block walls.
2. The quantity and distribution of imperfect blocks greatly impact an interlocking block wall's mean compressive strength. A high-quality wall, with fewer imperfect blocks, shows the highest mean compressive strength of 4.47 MPa at a COV of 0.1. Interestingly, a low-quality wall with more imperfect blocks could still outperform high-medium and medium–low quality walls in terms of compressive strength, especially when COV = 0.1, with the compressive strengths being 4.00 MPa, 3.38 MPa and 2.81 MPa, respectively. This phenomenon is attributed to the more uniform closure of gaps under compressive loading in the low-quality walls. In contrast, medium-quality walls suffer from non-uniform deformation and stress concentration, leading to lower compressive strengths.
3. The COV of block imperfection size has a marginal influence on the mean compressive strengths of high-quality and high-medium quality walls. Specifically, when COV increases from 0.1 to 0.5, the mean compressive strengths decrease slightly from 4.47 MPa to 4.40 MPa for high-quality walls, and from 3.38 MPa to 3.27 MPa for high-medium quality walls. In contrast, the mean compressive strength of

low-quality walls is more sensitive to the COV, significantly dropping from 4.00 MPa to 2.72 MPa as COV increases from 0.1 to 0.5.

4. Initial seating is obvious for medium–low and low-quality block walls under compressive load because of gap closure between imperfect blocks, and the seating displacement is prominent in the walls with relatively low-quality blocks.
5. The mean equivalent stiffnesses increase with the rise of COV of imperfection size distribution from 0.1 to 0.5 for high-quality, high-medium quality and medium–low quality walls. This is attributed to the significant decrease in displacements at the peak compressive loads, while the peak compressive load remains relatively unchanged. However, for low-quality walls, the mean equivalent stiffness demonstrates a decline with the increasing COV of block imperfection sizes due to the lower compressive strength, decreasing significantly from 92.9kN/mm to 72.6kN/mm as the COV of imperfection size increases from 0.1 to 0.5.
6. The mean linear stiffnesses of high-quality, high-medium and medium–low quality interlocking block walls undergo a significant decrease with the degradation of block quality. Specifically, the mean linear stiffnesses are found to be 511kN/mm, 320kN/mm, and 119kN/mm for high-quality, high-medium and medium–low quality walls respectively when COV = 0.1. This correlation is attributable to the influences of the number of imperfections exerting on the contact areas.

In conclusion, this study investigated the influence of block imperfections on the compressive properties of dry-stacked interlocking block walls. The findings demonstrate the significant impact of imperfections on crack patterns, load path, and compressive strength. The study also highlights the importance of imperfection size and quantity in determining the properties of the interlocking block walls. The results suggest that low-quality walls may have higher compressive strength than high-medium and medium–low quality walls due to the presence of gaps between blocks. However, the number and severity of localized block damage and failures increase as the quality of the block decreases, leading to lower compressive strengths.

Declaration of Competing Interest

The authors declare that they have no known competing financial interests or personal relationships that could have appeared to influence the work reported in this paper.

Acknowledgments

The authors would like to acknowledge the financial support from Australian Research Council for carrying out this study.

References

[1] Zhang X, Hao H, Zheng J, Hernandez F. The mechanical performance of concrete shear key for prefabricated structures. Adv Struct Eng 2021;24(2):291–306.
[2] Ramamurthy K, Kunhanandan Nambiar EK. Accelerated masonry construction review and future prospects. Prog Struct Eng Mater 2004;6(1):1–9.
[3] Wang G, Li Y, Zheng N, Ingham JM. Testing and modelling the in-plane seismic response of clay brick masonry walls with boundary columns made of precast concrete interlocking blocks. Eng Struct 2017;131:513–29.
[4] Kayaalp FB, Husem M. Enhancement of in-plane load-bearing capacity of masonry walls by using interlocking units. Earthquakes Struct 2022;22(5):475–85.
[5] Zhang X, Hao H, Li C, Do TV. Experimental study on the behavior of precast segmental column with domed shear key and unbonded Post-Tensioning tendon under impact loading. Eng Struct 2018;173:589–605.
[6] Zhang X, Hao H, Li C. Multi-hazard resistance capacity of precast segmental columns under impact and cyclic loading. Int J Protect Struct 2018;9(1):24–43.
[7] Lourenço PB, Pina-Henriques J. Validation of analytical and continuum numerical methods for estimating the compressive strength of masonry. Comput Struct 2006;84(29–30):1977–89.
[8] Sturm T, Ramos LF, Lourenço PB. Characterization of dry-stack interlocking compressed earth blocks. Mater Struct 2015;48(9):3059–74.
[9] Ngapeya GGC, Waldmann D, Scholzen F. Impact of the height imperfections of masonry blocks on the load bearing capacity of dry-stack masonry walls. Constr Build Mater 2018;165:898–913.
[10] Jaafar MS, Thanoon WA, Najm AMS, Abdulkadir MR, Abang Ali AA. Strength correlation between individual block, prism and basic wall panel for load bearing interlocking mortarless hollow block masonry. Constr Build Mater 2006;20(7):492–8.
[11] Al-Fakih A, Mohammed BS, Al-Shugaa MA, Al-Osta MA. Experimental investigation of dry-bed joints in rubberized concrete interlocking masonry. J Build Eng 2022;58:105048.
[12] Dorji S, Derakhshan H, Thambiratnam DP, Zahra T, Mohyeddin A. Behaviour and material properties of versaloc semi-interlocking mortarless masonry. Mater Struct 2023;56(1).
[13] Zahra T, Dorji J, Thamboo J, Cameron N, Asad M, Kasinski W, et al. Behaviour of reinforced mortarless concrete masonry panels under axial compression: An experimental and analytical study. Constr Build Mater 2023;377:131097.
[14] Zahra T, Dhanasekar M. Characterisation and strategies for mitigation of the contact surface unevenness in dry-stack masonry. Constr Build Mater 2018;169:612–28.
[15] Thanoon WAM, Alwathaf AH, Noorzaei J, Jaafar MS, Abdulkadir MR. Finite element analysis of interlocking mortarless hollow block masonry prism. Comput Struct 2008;86(6):520–8.
[16] Martínez M, Atamturktur S, Ross B, Thompson J. Assessing the Compressive Behavior of Dry-Stacked Concrete Masonry with Experimentally Informed Numerical Models. J Struct Eng 2018;144(7).
[17] Fundi, S.I., J.W. Kaluli, and J. Kinuthia, *Finite element modelling of interlocking stabilized laterite soil block walls.* SN Applied Sciences, 2021. **3**(2): p. 1-11.
[18] Martínez M, Atamturktur S. Experimental and numerical evaluation of reinforced dry-stacked concrete masonry walls. J Build Eng 2019;22:181–91.
[19] Shi T, et al. Experimental and numerical investigation on the compressive properties of interlocking blocks. Eng Struct 2021;228:111561.
[20] Huamani K, Enciso R, Gonzales M, Zavaleta D, Aguilar R. Experimental and numerical evaluation of a stackable compressed earth block masonry system: Characterization at cyclic shear loads. J Build Eng 2022;60:105139.
[21] Al-Fakih A, Al-Osta MA. Finite Element Analysis of Rubberized Concrete Interlocking Masonry under Vertical Loading. Materials (Basel) 2022;15(8):2858.
[22] Xie G, Zhang X, Hao H, Bi K, Lin Y. Response of reinforced mortar-less interlocking brick wall under seismic loading. Bull Earthq Eng 2022;20(11):6129–65.
[23] Xie G, Zhang X, Hao H, Shi T, Cui L, Thomas J. Behaviour of reinforced mortarless interlocking brick wall under cyclic loading. Eng Struct 2023;283:115890.
[24] Andreev K, Sinnema S, Rekik A, Allaoui S, Blond E, Gasser A. Compressive behaviour of dry joints in refractory ceramic masonry. Constr Build Mater 2012;34:402–8.
[25] Lin K, Totoev Y, Liu H, Wei C. Experimental characteristics of dry stack masonry under compression and shear loading. Materials 2015;8(12):8731–44.
[26] Kaushik HB, Rai DC, Jain SK. Stress-strain characteristics of clay brick masonry under uniaxial compression. J Mater Civ Eng 2007;19(9):728–39.
[27] Briga-Sá A, Silva RA, Gaibor N, Neiva V, Leitão D, Miranda T. Mechanical Characterization of Masonry Built with iCEBs of Granite Residual Soils with Cement-Lime Stabilization. Buildings 2022;12(9):1419.
[28] Jaafar MS, Alwathaf AH, Thanoon WA, Noorzaei J, Abdulkadir MR. Behaviour of interlocking mortarless block masonry. Proc Inst Civ Eng - Constr Mater 2006;159(3):111–7.
[29] Chan C, Hover KC, Folliard KJ. Spatial variations in material properties of segmental retaining wall (SRW) units, part II: sampling considerations for absorption tests. J ASTM Int 2005;2(2):1–18.
[30] Lawrence, S. *Random variations in brickwork properties*. in *Proc., 7th Int. Brick Masonry Conf*. 1985.
[31] Stewart MG. Spatial variability of pitting corrosion and its influence on structural fragility and reliability of RC beams in flexure. Struct Saf 2004;26(4):453–70.
[32] Zhu F, Zhou Q, Wang F, Yang Xu. Spatial variability and sensitivity analysis on the compressive strength of hollow concrete block masonry wallettes. Constr Build Mater 2017;140:129–38.
[33] Stewart M, Lawrence S. Model error, structural reliability and partial safety factors for structural masonry in compression. Masonry International 2007;20(3):107–16.
[34] Standard, A., *AS 3700: masonry structures*. 2001, Sydney.
[35] Heffler L, et al. Statistical analysis and spatial correlation of flexural bond strength for masonry walls. Masonry Int 2008;21(2):59–70.
[36] Li J, Masia MJ, Stewart MG, Lawrence SJ. Spatial variability and stochastic strength prediction of unreinforced masonry walls in vertical bending. Eng Struct 2014;59:787–97.
[37] Fyfe A, Middleton J, Pande G. Numerical evaluation of the influence of some workmanship defects on the partial factor of safety (GAMMA M) for masonry. Masonry Int 2000;13(2):48–53.
[38] Stewart MG, Lawrence S. Structural reliability of masonry walls in flexure. Masonry Int 2002;15(2):48–52.
[39] Gooch LJ, Masia MJ, Stewart MG. Application of stochastic numerical analyses in the assessment of spatially variable unreinforced masonry walls subjected to in-plane shear loading. Eng Struct 2021;235:112095.
[40] Dyskin A, Estrin Y, Pasternak E. Topological interlocking materials. Archit Mater Nat Eng: Archimats 2019:23–49.
[41] Dyskin AV, Estrin Y, Pasternak E, Khor HC, Kanel-Belov AJ. Fracture resistant structures based on topological interlocking with non-planar contacts. Adv Eng Mater 2003;5(3):116–9.
[42] ABAQUS, A., *6.14, Dassault Systèmes Simulia Corp.* Provid. RI, USA, 2014.

[43] Shi T, et al. Experimental and numerical studies of the shear resistance capacities of interlocking blocks. J Build Eng 2021;44:103230.
[44] Simulia, *Abaqus Analysis User's Guide, Version 6.14*. 2014, Dassault Systemes Providence, RI.
[45] Gorst N, et al. Friction in temporary works. Res Rep 2003:71.
[46] EN, B., *1052-1 (1999) British Standard. Methods of test for masonry—Part 1: Determination of compressive strength. CEN European Committee for Standardization. Central Secretariat: rue de Stassart 36, B-1050 Brussels, September, 1998*.
[47] Shields MD, Teferra K, Hapij A, Daddazio RP. Refined stratified sampling for efficient Monte Carlo based uncertainty quantification. Reliab Eng Syst Saf 2015; 142:310–25.
[48] Tabbakhha M, Modaressi-Farahmand-Razavi A. Analyzing the effect of workmanship quality on performance of unreinforced masonry walls through numerical methods. Comput Struct 2016;167:1–14.